



HAL
open science

Determining the isotopic composition of elements from the electrospray ionization mass spectra of their chemical species

Evelyne Blanchard, Eduardo Paredes, Anaïs Rincel, Anthony Nonell, Frédéric Chartier, Carole Bresson

► **To cite this version:**

Evelyne Blanchard, Eduardo Paredes, Anaïs Rincel, Anthony Nonell, Frédéric Chartier, et al.. Determining the isotopic composition of elements from the electrospray ionization mass spectra of their chemical species. *Journal of Analytical Atomic Spectrometry*, 2021, 36 (4), pp.758. 10.1039/d0ja00471e . cea-03203350

HAL Id: cea-03203350

<https://cea.hal.science/cea-03203350v1>

Submitted on 20 Apr 2021

HAL is a multi-disciplinary open access archive for the deposit and dissemination of scientific research documents, whether they are published or not. The documents may come from teaching and research institutions in France or abroad, or from public or private research centers.

L'archive ouverte pluridisciplinaire **HAL**, est destinée au dépôt et à la diffusion de documents scientifiques de niveau recherche, publiés ou non, émanant des établissements d'enseignement et de recherche français ou étrangers, des laboratoires publics ou privés.

JAAS

Journal of Analytical Atomic Spectrometry

Accepted Manuscript

This article can be cited before page numbers have been issued, to do this please use: E. Blanchard, E. Paredes Paredes, A. Rincel, A. Nonell, F. Chartier and C. Bresson, *J. Anal. At. Spectrom.*, 2021, DOI: 10.1039/D0JA00471E.



This is an Accepted Manuscript, which has been through the Royal Society of Chemistry peer review process and has been accepted for publication.

Accepted Manuscripts are published online shortly after acceptance, before technical editing, formatting and proof reading. Using this free service, authors can make their results available to the community, in citable form, before we publish the edited article. We will replace this Accepted Manuscript with the edited and formatted Advance Article as soon as it is available.

You can find more information about Accepted Manuscripts in the [Information for Authors](#).

Please note that technical editing may introduce minor changes to the text and/or graphics, which may alter content. The journal's standard [Terms & Conditions](#) and the [Ethical guidelines](#) still apply. In no event shall the Royal Society of Chemistry be held responsible for any errors or omissions in this Accepted Manuscript or any consequences arising from the use of any information it contains.

Determining the isotopic composition of elements from the electrospray ionization mass spectra of their chemical species

View Article Online
DOI: 10.1039/D0JA00471E

AUTHORS: E. Blanchard^{a,b,#}, E. Paredes^{a,£}, A. Rincel^a, A. Nonell^a, F. Chartier^c, C. Bresson^{a*}

^a Université Paris-Saclay, CEA, Service d'Etudes Analytiques et de Réactivité des Surfaces F-91191, Gif-sur-Yvette, France

^b Sorbonne Université, F-75005 Paris, France

^c Université Paris-Saclay, CEA, Département de Physico-Chimie F-91191 Gif-sur-Yvette, France

Current address:

[#] Normandie Univ, UNIROUEN, Ecodiv, 76000 Rouen, France

[£] Departament de Dinàmica de la Terra i de l'Oceà, Facultat de Ciències de la Terra, Universitat de Barcelona, 08028 Barcelona, Spain

*** CORRESPONDING AUTHOR:**

Carole BRESSON

Tel: +33 (0)169088348

E-mail address: carole.bresson@cea.fr

KEYWORDS:

Isotopic composition, deconvolution, lanthanides, ESIMS, electrospray ionization mass spectrometry, chemical species, speciation

ABSTRACT:

View Article Online

DOI: 10.1039/D0JA00471E

Electrospray ionization mass spectrometry (ESIMS) is traditionally used to analyse organic molecules, but can also be used to carry out elemental speciation studies. The challenge is here to determine the isotopic composition of elements contained in chemical species by this technique, in addition to their quantification and structural characterisation. In the present work, we determined by ESIMS the isotope ratios of samarium (Sm) and neodymium (Nd) involved in complexes containing polyaminocarboxylic acids, namely EDTA and DTPA. To this end, we developed a user-friendly deconvolution method to remove the ligand isotopic contributions from the abundance ratios measured in the ESI mass spectra of the complexes, and thus obtaining the isotopic composition of the free lanthanides. By applying the deconvolution method to EDTA complexes containing natural and enriched samarium, we obtained the ^{nat}Sm and the $^{147-149}\text{Sm}$ isotopic composition directly from the mass spectra of the chemical species recorded by commercial ESI mass spectrometers, equipped with a triple quadrupole analyser (QqQ) or a linear ion trap (LIT). The isotopic composition of ^{nat}Sm and $^{147-149}\text{Sm}$ were determined with a trueness better than 3.5% and 2% by ESI-QqQ-MS and better than 1% and 2% by ESI-LIT-MS, with a repeatability globally better than 3% at $k=2$, for isotopes of relative abundances greater than 1% in samples. This method was successfully applied to determine ^{nat}Nd and ^{nat}Sm isotopic compositions from $^{nat}\text{Nd-EDTA}$, $^{nat}\text{Sm-DTPA}$ and $^{nat}\text{Nd-DTPA}$ mass spectra.

1 Speciation analysis of an element refers to the identification and structural characterisation of
2 different chemical species in which it is contained, as well as the oxidation state identification, the
3 quantification and isotopic characterisation of the element in each species.¹ The isotopic composition
4 of elements incorporated in chemical species is becoming increasingly more prevalent in the field of
5 speciation.² Isotope ratio variations can provide important information on the origin of the elements
6 or on chemical, physical and biological processes in which these elements are involved. For nuclear
7 applications, quantifying and determining the isotopic composition of radioelements have a major
8 impact on issues such as nuclear fuel recycling or waste storage.³ The coupling of liquid
9 chromatography to electrospray ionization mass spectrometry (LC-ESIMS) makes it possible to
10 structurally characterize and quantify chemical species after their separation.^{4,5} However, the ability
11 to directly determine the isotopic compositions of elements contained in species by ESIMS remains
12 to be assessed to obtain comprehensive speciation information by this technique on its own. This
13 study focuses on the measurement of natural and non-natural lanthanide's (Ln) isotopic composition
14 contained in Ln-polyaminocarboxylic acid species by ESIMS. These measurements are of great
15 interest in the field of speciation analysis of elements contained in species that can be found in
16 nuclear applications.⁶ Moreover, obtaining structural, elemental and isotopic data on chemical
17 species in a single step is beneficial since it not only reduces costs and analysis time, but also
18 handling and exposure times in the case of radioactive samples.

19 Although articles dealing with the study of metal-ligand interactions by ESIMS in solution and solid
20 states are reported in the literature,⁷⁻⁹ very few studies are to our knowledge dedicated to the
21 determination of the isotopic composition of elements by ESIMS.¹⁰⁻¹² In general, these isotopic
22 measurements were performed with prototypes or modified instruments and very often starting with
23 inorganic metallic compounds such as nitrate or fluoride derivatives.¹⁰⁻¹² Pioneering studies were
24 performed in the 1990s using a modified quadrupole ICPMS (ICPMS-Q) in which the source was
25 replaced by an electrospray ionization source.¹⁰ Measurements performed with silver nitrate and
26 thallium acetate led to $^{107}\text{Ag}/^{109}\text{Ag}$ and $^{205}\text{Tl}/^{203}\text{Tl}$ ratio determination. From the 2000s, ESIMS
27 instruments with modified sources were tested for isotopic measurements. A quadrupole mass
28 spectrometer in which the probe, the injection system and the counter electrode were modified, was
29 used to measure boron isotope ratios, $^{10}\text{B}/^{11}\text{B}$.¹¹ In order to avoid hydride interferences, boron

1 species were converted into a complex containing a monoisotopic ligand, namely BF_4^- by adding
2 hydrofluoric acid to the sample. However, it must be noticed that this strategy induces the
3 modification of the initial speciation of the element in the sample. The analysis of uranium (U) isotopic
4 composition was performed with a linear ion trap mass spectrometer equipped with a homemade
5 extractive electrospray source, suitable for the analysis of samples in complex matrices.¹² The
6 approach involved performing tandem mass spectrometry experiments on uranyl nitrate compounds
7 to obtain product ions, in order to determine the most accurate $^{235}\text{U}/^{238}\text{U}$ isotope ratio. At each
8 fragmentation step, the abundance ratio of product ions containing the ^{235}U and ^{238}U isotopes was
9 measured and compared against the theoretical $^{235}\text{U}/^{238}\text{U}$ isotope ratio. Through the MS^4
10 fragmentation step, the abundance ratio of $^{235}\text{UO}_7\text{N}_1\text{H}_2/^{238}\text{UO}_7\text{N}_1\text{H}_2$ could be obtained. However,
11 even by using tandem mass spectrometry to fragment the species, the isotopic contributions of the
12 remaining ligand atoms hampered the direct measurement of the element isotope ratios by ESIMS.
13 Although all these studies allowed to obtain isotopic measurements with satisfying performance, the
14 isotopic composition of the free elements was never reached directly.

15 In our case, the Ln isotopic pattern in the chemical species differ from the single-element isotopic
16 composition due to the contributions of several atoms from the ligand, being EDTA or DTPA, no less
17 than twelve hydrogen (H) atoms, ten carbon (C) atoms, two nitrogen (N) atoms and eight oxygen
18 (O) atoms. In order to determine the Ln isotopic composition from the ESI mass spectra of the
19 associated chemical species, our strategy was to develop a user-friendly deconvolution method to
20 remove the H, C, N and O isotopic contributions from these spectra and thus directly determine the
21 free lanthanide isotopic composition, without needing to perform several fragmentations of the
22 chemical species by tandem mass spectrometry. By applying this deconvolution method, we
23 determined the natural and the non-natural isotopic composition of Sm ($^{\text{nat}}\text{Sm}$ and $^{147-149}\text{Sm}$) directly
24 from the experimental mass spectra of the EDTA-containing complexes ($^{\text{nat}}\text{Sm-EDTA}$ and $^{147-149}\text{Sm-EDTA}$)
25 recorded by commercial QqQ and LIT ESIMS instruments. We further applied the
26 deconvolution method to other Ln species containing Nd or DTPA, i.e. $^{\text{nat}}\text{Nd-EDTA}$, $^{\text{nat}}\text{Sm-DTPA}$ and
27 $^{\text{nat}}\text{Nd-DTPA}$. In each case, the performance of the method was evaluated at each step in terms of its
28 trueness and precision.

1 It must be pointed out that only some commercial instruments equipped with high resolution or ultra
2 high resolution analysers could allow eliminating the need of deconvolution, but these instruments
3
4
5
6 are only available in some laboratories dedicated to specific applications. The great advantage of
7
8 the approach that we developed is that it is simply applicable for any users and for any metallic
9
10 complexes, by implementing basic spreadsheets using data from the ESI mass spectra of the
11
12 chemical species, obtained with low resolution mass spectrometers widely available in analytical
13
14 chemistry laboratories.
15
16
17

18 19 20 21 22 23 24 25 26 27 28 29 30 31 32 33 34 35 36 37 38 39 40 41 42 43 44 45 46 47 48 49 50 51 52 53 54 55 56 57 58 59 60

EXPERIMENTAL SECTION

Chemicals and samples

Ethylenediaminetetraacetic acid tetrasodium salt dihydrate (EDTA, $C_{10}H_{12}O_8N_2Na_4 \cdot 2H_2O$, purity \geq 99.5%) and diethylenetriaminepentaacetic acid (DTPA, $C_{14}H_{23}O_{10}N_3$, purity \geq 98%) were supplied by Sigma Aldrich (Saint Quentin Fallavier, France). Ultrapure water (resistivity 18.2 M Ω .cm) was obtained from a Milli-Q water purification system (Millipore, Guyancourt, France). Acetonitrile (CH_3CN , LC-MS grade), formic acid (Normapur grade), ammonium acetate ($CH_3CO_2NH_4$, Normapur grade) and ammonia solution 25% were purchased from VWR Prolabo (Briare-le-Canal, France). HNO_3 65% (Merck Company, France) was distilled with an evapoclean system from Analab (France). This acid was used to prepare HNO_3 at 2% w/w in ultrapure water. Natural samarium (^{nat}Sm) and natural neodymium (^{nat}Nd) standard solutions at 1000 $\mu g mL^{-1}$ in HNO_3 2% w/w were provided by Spex Certiprep Group (Longjumeau, France). The isotopic compositions of ^{nat}Sm and ^{nat}Nd were determined by thermal ionization mass spectrometry (TIMS) (VG 354, VG Elemental); this data is provided in Table 1.¹³ A double spike $^{147-149}Sm$ solution was prepared beforehand by dissolution in nitric acid of two Sm_2O_3 powders, enriched in ^{147}Sm (94.40%) and in ^{149}Sm (95.13%), to obtain a $^{147}Sm/^{149}Sm$ isotope ratio close to one.¹⁴ The concentration of HNO_3 in this enriched stock solution was around 4.8 mol L^{-1} and the total Sm concentration of 9.75×10^{-4} mol L^{-1} (144.3 $\mu g mL^{-1}$). The isotopic composition of the double spike was characterized by TIMS (Isoprobe-T mass spectrometer, IsotopX Ltd) and is given in Table 1.¹⁴

Table 1: Reference Sm and Nd isotope ratios obtained by TIMS and associated relative abundances in ^{nat}Sm ¹³, $^{147-149}Sm$ ¹⁴ and ^{nat}Nd ¹³; the values between brackets correspond to the expanded

uncertainty ($k=2$). The ^{nat}Sm and ^{nat}Nd isotope ratios were internally normalized to $^{147}\text{Sm}/^{149}\text{Sm}=1.08680(32)$ and to $^{146}\text{Nd}/^{144}\text{Nd}=0.72333(16)$. The uncertainty of the relative abundance of ^{nat}Sm , $^{147-149}\text{Sm}$ and ^{nat}Nd isotopes was calculated with the Kragten method.¹⁵

	Isotope ratio	Measured	Isotope	Relative abundance (%)
^{nat}Sm	$^{144}\text{Sm}/^{150}\text{Sm}$	0.41943(59)	^{144}Sm	3.096(4)
	$^{147}\text{Sm}/^{150}\text{Sm}$	2.0365(13)	^{147}Sm	15.034(5)
	$^{148}\text{Sm}/^{150}\text{Sm}$	1.52568(87)	^{148}Sm	11.263(3)
	$^{149}\text{Sm}/^{150}\text{Sm}$	1.8739(10)	^{149}Sm	13.833(3)
	$^{152}\text{Sm}/^{150}\text{Sm}$	3.6173(23)	^{150}Sm	7.382(4)
	$^{154}\text{Sm}/^{150}\text{Sm}$	3.0733(21)	^{152}Sm	26.704(8)
			^{154}Sm	22.688(8)
$^{147-149}\text{Sm}$	$^{144}\text{Sm}/^{147}\text{Sm}$	0.00094(4)	^{144}Sm	0.047(2)
	$^{148}\text{Sm}/^{147}\text{Sm}$	0.05343(31)	^{147}Sm	50.005(51)
	$^{149}\text{Sm}/^{147}\text{Sm}$	0.9035(18)	^{148}Sm	2.672(15)
	$^{150}\text{Sm}/^{147}\text{Sm}$	0.02526(8)	^{149}Sm	45.178(46)
	$^{152}\text{Sm}/^{147}\text{Sm}$	0.01133(4)	^{150}Sm	1.263(3)
	$^{154}\text{Sm}/^{147}\text{Sm}$	0.00536(3)	^{152}Sm	0.567(2)
			^{154}Sm	0.268(1)
^{nat}Nd	$^{142}\text{Nd}/^{144}\text{Nd}$	1.13966(28)	^{142}Nd	27.109(6)
	$^{143}\text{Nd}/^{144}\text{Nd}$	0.51097(10)	^{143}Nd	12.155(3)
	$^{145}\text{Nd}/^{144}\text{Nd}$	0.34874(4)	^{144}Nd	23.787(3)
	$^{146}\text{Nd}/^{144}\text{Nd}$	0.72333	^{145}Nd	8.296(2)
	$^{148}\text{Nd}/^{144}\text{Nd}$	0.24302(20)	^{146}Nd	17.206(4)
	$^{150}\text{Nd}/^{144}\text{Nd}$	0.23821(14)	^{148}Nd	5.781(5)
			^{150}Nd	5.666(4)

Two stock solutions of EDTA were prepared at 5×10^{-3} mol L⁻¹ and 1.76×10^{-3} mol L⁻¹ and a stock solution of DTPA was also prepared at 5×10^{-3} mol L⁻¹ by dissolution of the corresponding powder in ultrapure water.

A 5×10^{-3} mol L⁻¹ ($751.8 \mu\text{g mL}^{-1}$) ^{nat}Sm stock solution was prepared by dilution of the ^{nat}Sm standard solution in ultrapure water. This stock solution was mixed with the 5×10^{-3} mol L⁻¹ EDTA stock solution

1 to obtain a Sm: EDTA ratio of 1:1.2, with $[\text{natSm}] = 2.27 \times 10^{-3} \text{ mol L}^{-1}$. This solution was used to
2
3 develop the deconvolution method.

4
5 A $8.34 \times 10^{-4} \text{ mol L}^{-1}$ ($125.5 \text{ } \mu\text{g mL}^{-1}$) natSm stock solution was prepared by dilution of the natSm
6
7 standard solution in a $4.8 \text{ mol L}^{-1} \text{ HNO}_3$ solution. The two natSm and $^{147-149}\text{Sm}$ stock solutions were
8
9 evaporated and then redissolved in HNO_3 (2% w/w) to obtain a total Sm concentration of $5 \times 10^{-3} \text{ mol}$
10
11 L^{-1} ($751.8 \text{ } \mu\text{g mL}^{-1}$) for natSm and $5.85 \times 10^{-3} \text{ mol L}^{-1}$ ($866 \text{ } \mu\text{g mL}^{-1}$) for $^{147-149}\text{Sm}$. Then both solutions
12
13 were mixed with the $1.76 \times 10^{-3} \text{ mol L}^{-1}$ EDTA stock solution to obtain a natSm : EDTA ratio of 1:1.2,
14
15 with $[\text{natSm}] = 1.1 \times 10^{-3} \text{ mol L}^{-1}$ and a $^{147-149}\text{Sm}$:EDTA ratio of 1:1, with $[\text{natSm}] = 1.3 \times 10^{-3} \text{ mol L}^{-1}$.
16
17 These two solutions were used to validate the deconvolution method.

18
19 In the same manner, a $5 \times 10^{-3} \text{ mol L}^{-1}$ ($721.2 \text{ } \mu\text{g mL}^{-1}$) natNd stock solution was prepared by dilution
20
21 of the corresponding standard solution in ultrapure water. An appropriate volume of natLn (Ln = Nd
22
23 or Sm) stock solutions were mixed with stock solution of EDTA or DTPA to obtain an Ln-
24
25 polyaminocarboxylic acid ratio of 1:1.2, with $[\text{natLn}] = 2.27 \times 10^{-3} \text{ mol L}^{-1}$. These solutions were used
26
27 to apply the deconvolution method to natNd-EDTA , natSm-DTPA and natNd-DTPA species.

28
29 In all cases, the pH of these solutions was adjusted to 3.2 by adding a 25% ammonia solution, in
30
31 order to obtain common pH in the aqueous back-extraction phases of spent nuclear fuel treatment
32
33 processes. In view of the future coupling of chromatography to ESIMS, the working samples were
34
35 prepared by diluting the previous solutions in a mobile phase made of 70/30 (v/v) acetonitrile/water,
36
37 0.5% formic acid and $15 \times 10^{-3} \text{ mol L}^{-1}$ of ammonium acetate, to reach a final Ln concentration of 10^{-4}
38
39 mol L^{-1} ($15 \text{ } \mu\text{g mL}^{-1}$ for Sm and $14.5 \text{ } \mu\text{g mL}^{-1}$ for Nd).
40
41
42
43
44
45

46 ESIMS instrumentation

47
48 We used a TSQ quantum quadrupole mass spectrometer (ESI-QqQ-MS, Thermo Fisher Scientific,
49
50 USA) equipped with an H-ESI-II ionization source and a triple quadrupole analyser. We also used a
51
52 LTQ Velos Pro mass spectrometer (ESI-LIT-MS, Thermo Fisher Scientific, USA) equipped with an
53
54 H-ESI-II ionization source and a linear ion trap analyser. The samples were continuously injected
55
56 into the spectrometers at a flow rate of $10 \text{ } \mu\text{L min}^{-1}$. All ESIMS spectra were recorded in negative
57
58 ionization mode and in MS mode.
59
60

For both instruments, the acquisition parameters leading to the best performance for $^{nat}\text{Sm-EDTA}$ complex were selected (Table 2).

View Article Online
DOI: 10.1039/D0JA00471E

Table 2: setting parameters selected for the experiments

	ESI-QqQ-MS TSQ quantum	ESI-LIT-MS LTQ Velos Pro
Spray voltage	-3.7kV	
Capillary transfer temperature (°C)	280	
Vaporisation temperature (°C)	90	
Sheath gas (a.u.)	10	
Auxiliary gas (a.u.)	10	5
Skimmer offset (V)	0	-
S-lens (%)	-	70
Fragmentation in source (eV)	-	40
Scan number	100	
Scan time (s)	0.7	-
FWHM / Scan rate (kDa s ⁻¹)	0.5/ -	0.35 / 10

These parameters were also applied for abundance ratio measurements in $^{147-149}\text{Sm-EDTA}$, $^{nat}\text{Nd-EDTA}$, $^{nat}\text{Sm-DTPA}$ and $^{nat}\text{Nd-DTPA}$. With the ESI-QqQ-MS and the ESI-LIT-MS, the abundance ratios of complexed lanthanides were determined based on the average of ten measurements for all samples containing lanthanides with natural isotopic composition and on the average of three series of ten measurements for the sample containing samarium with non-natural isotopic composition.

A $^{nat}\text{Sm-EDTA}$ solution was used as the control standard at the beginning and end of the analytical sessions to measure $^{147-149}\text{Sm-EDTA}$ abundance ratios, in order to correct potential instrumental mass bias values. This standard was prepared in the same manner as the enriched $^{147-149}\text{Sm-EDTA}$ sample, by respecting the initial composition of the matrix (HNO_3 4.8 mol L⁻¹). No instrumental mass bias was observed during these measurement sessions but background signal variations were observed in the control standard. These background signal variations were corrected on the enriched sample by normalizing and subtracting them from the intensities measured on the control standard.

RESULTS AND DISCUSSION

Development of the deconvolution method

This method was developed with ^{nat}Sm -EDTA and further applied to the other Ln complexes. Briefly, we first calculated the theoretical isotopic pattern of ^{nat}Sm -EDTA by convolution. Based on this initial convolution data, we then defined the matrix of the isotopic contributions of the ligand atoms H, C, N and O. By combining this latter matrix with the measured intensities in the mass spectra of ^{nat}Sm -EDTA, we established a system of equations to determine the ^{nat}Sm isotopic composition. Among the available convolution methods,¹⁶ we used the readily implemented Yerger's polynomial method¹⁷ taking into account the stoichiometry of the complex and the relative isotopic abundances using both International Union of Pure and Applied Chemistry (IUPAC) data for H, C, N and O¹⁸ and TIMS data measured at the laboratory for ^{nat}Sm ¹³ (Table 1 and Figure 1b). By applying the Yerger's convolution method, we calculated the theoretical mass spectrum of negatively monocharged ^{nat}Sm -EDTA (Figure 1c).

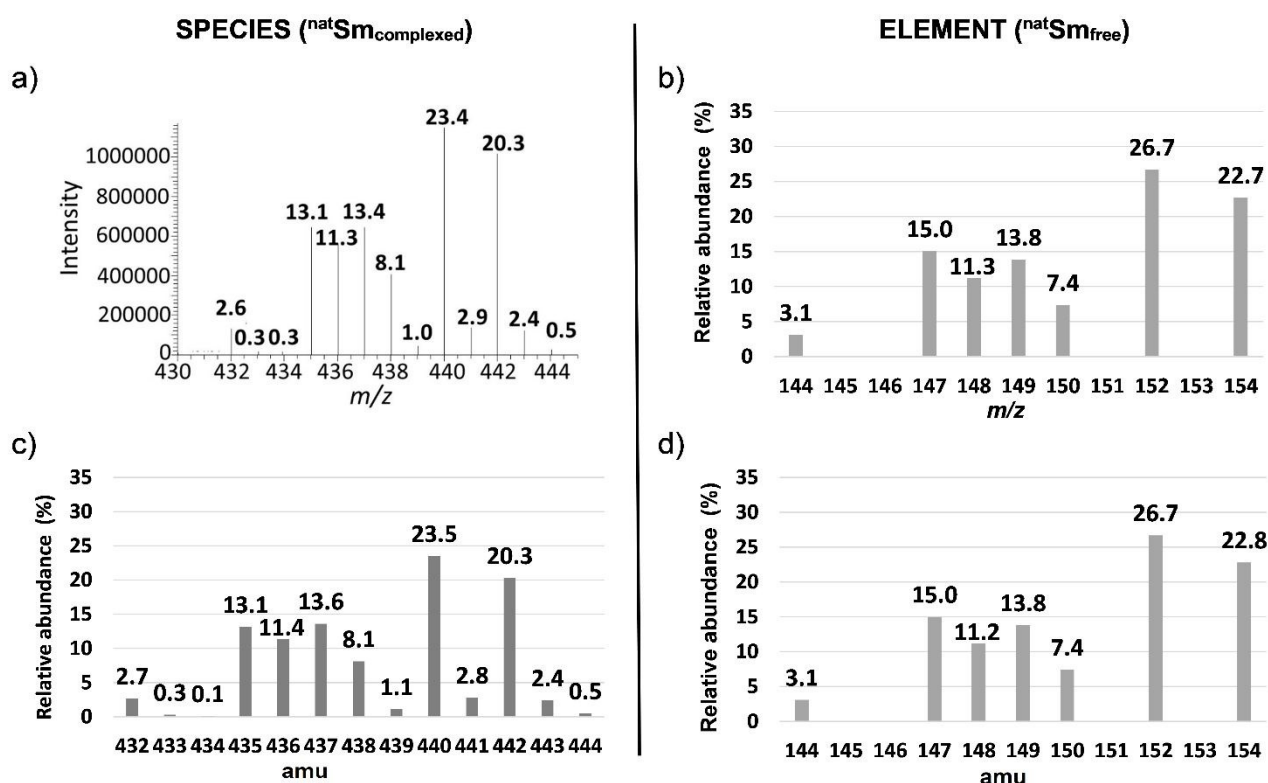


Figure 1: Isotopic patterns of ^{nat}Sm -EDTA and ^{nat}Sm a) experimental mass spectrum of ^{nat}Sm -EDTA recorded by ESI-LIT-MS in full scan mode, b) reference ^{nat}Sm isotopic pattern obtained by TIMS¹³,

c) ^{nat}Sm -EDTA isotopic pattern calculated with the Yergey convolution method¹⁷ d) ^{nat}Sm isotopic pattern obtained by deconvolution of the experimental ESI mass spectrum of ^{nat}Sm -EDTA

View Article Online
DOI: 10.1039/D0JA00471E

Except for Sm for which the stoichiometry is one, we calculated the atomic abundance of each isotopic permutation for each element using Eq. 1:

$$A = \frac{n!}{a!b!c!\dots} r_1^a r_2^b r_3^c \dots \quad (\text{Eq. 1})$$

Where A: atomic abundance for each permutation

n: number of atoms of the element

a, b, c, etc: number of isotopes of the element in the permutation

r_1, r_2, r_3, \dots : atomic abundance of each isotope of the element

For example, one of the permutations of C_{10} is $^{12}\text{C}_8^{13}\text{C}_2$, leading to the atomic abundance of 4727 ppm (Figure 2):

$$A_{^{12}\text{C}_8^{13}\text{C}_2} = \frac{10!}{8!2!} \times 0.9893^8 \times 0.0107^2 = 4.727 \times 10^{-3}$$

Carbon				
Number of ^{12}C	Number of ^{13}C	m/z	Abundance	Abundance (ppm)
10	0	120	0.898	898008
9	1	121	0.097	97126
8	2	122	0.005	4727
7	3	123	1.10^{-4}	136
6	4	124	3.10^{-6}	3
5	5	125	3.10^{-8}	3.10^{-2}

Hydrogen				
Number of ^1H	Number of ^2H	m/z	Abundance	Abundance (ppm)
12	0	12	0.999	998621
11	1	13	0.001	1378
10	2	14	9.10^{-7}	0.9

Figure 2: atomic abundance of carbon and hydrogen isotopic permutations for deprotonated EDTA ($\text{C}_{10}\text{H}_{12}\text{N}_2\text{O}_8$)

We disregarded all permutations with abundances lower than 10 ppm for the next step of our study as they have a negligible impact on our calculations.

In a second step, the abundance of each permutation for $^{nat}\text{Sm-EDTA}$ was determined. It corresponds to the product of the abundance of the isotopic permutations of each element, calculated in the first step, by respecting the stoichiometry of the species. For example, the abundance of the $^{148}\text{Sm}^{12}\text{C}_8^{13}\text{C}_2^1\text{H}_{12}^{14}\text{N}_2^{16}\text{O}_7^{18}\text{O}_1$ permutation at m/z 440 was calculated according to Eq. 2, resulting in 8.51×10^{-6} :

$$A^{148}\text{Sm}^{12}\text{C}_8^{13}\text{C}_2^1\text{H}_{12}^{14}\text{N}_2^{16}\text{O}_7^{18}\text{O}_1 = A^{148}\text{Sm} \times A^{12}\text{C}_8^{13}\text{C}_2 \times A^1\text{H}_{12} \times A^{14}\text{N}_2 \times A^{16}\text{O}_7^{18}\text{O}_1 \quad (\text{Eq. 2})$$

The third step consisted in summing the combined abundances of all the previous calculated permutations for each m/z ratio and Sm isotope. Table 3 gives the results in matrix form, with the m/z ratios of the $^{nat}\text{Sm-EDTA}$ in columns and the ^{nat}Sm isotopes in rows.

Table 3: Relative abundances (in %) for each m/z ratio in $^{nat}\text{Sm-EDTA}$ calculated with the Yergey convolution method¹⁷ using the relative isotopic abundances of H, C, N and O from IUPAC¹⁸ and from TIMS data for ^{nat}Sm ¹³

Element	Species																			
	432	433	434	435	436	437	438	439	440	441	442	443	444	445	446	447	448	449	450	451
^{144}Sm	2.7×10^{-2}	3×10^{-3}	1×10^{-3}	5.9×10^{-5}	6.2×10^{-6}	4.7×10^{-7}	2.1×10^{-8}	6.4×10^{-10}	4.6×10^{-12}	1.2×10^{-14}	8.9×10^{-18}									
^{147}Sm				0.131	1.6×10^{-2}	0.003	2.9×10^{-4}	3.0×10^{-5}	2.3×10^{-6}	1.0×10^{-7}	3.1×10^{-9}	2.2×10^{-11}	5.7×10^{-14}	4.3×10^{-17}						
^{148}Sm					9.8×10^{-2}	1.2×10^{-2}	2×10^{-3}	2.1×10^{-4}	2.2×10^{-5}	1.7×10^{-6}	7.6×10^{-8}	2.3×10^{-9}	1.7×10^{-11}	4.3×10^{-14}	3.3×10^{-17}					
^{149}Sm						0.121	1.4×10^{-2}	3×10^{-3}	2.6×10^{-4}	2.8×10^{-5}	2.1×10^{-6}	9.3×10^{-8}	2.9×10^{-9}	2.1×10^{-11}	5.2×10^{-14}	4.0×10^{-17}				
^{150}Sm							0.064	8×10^{-3}	1×10^{-3}	1.4×10^{-4}	1.5×10^{-5}	1.1×10^{-6}	5.0×10^{-8}	1.5×10^{-9}	1.1×10^{-11}	2.8×10^{-14}	2.1×10^{-17}			
^{152}Sm									0.233	2.8×10^{-2}	5×10^{-3}	1×10^{-3}	5.3×10^{-5}	4.1×10^{-6}	1.8×10^{-7}	5.5×10^{-9}	4.0×10^{-11}	1.0×10^{-13}	7.7×10^{-17}	
^{154}Sm											0.198	2.4×10^{-2}	5×10^{-3}	4.3×10^{-4}	4.5×10^{-5}	3.4×10^{-6}	1.5×10^{-7}	4.7×10^{-9}	3.4×10^{-11}	8.6×10^{-14}
Total	0.03	0.00	0.00	0.13	0.11	0.14	0.08	0.01	0.23	0.03	0.20	0.02	0.00	0.00	0.00	0.00	0.00	0.00	0.00	0.00
Abundance (%)	2.7	0.3	0.1	13.1	11.4	13.6	8.1	1.1	23.5	2.8	20.3	2.4	0.5	0.0	0.0	0.0	0.0	0.0	0.0	0.0

1
2 By way of example, in the cell corresponding to m/z 440 and ^{148}Sm , the abundances of all the
3 permutations corresponding to this m/z with ^{148}Sm (e.g. $\text{A}^{148}\text{Sm}^{12}\text{C}_8^{13}\text{C}_2^{1}\text{H}_{12}^{14}\text{N}_2^{16}\text{O}_7^{18}\text{O}_1$ and
4 $\text{A}^{148}\text{Sm}^{12}\text{C}_9^{13}\text{C}_1^{1}\text{H}_{12}^{14}\text{N}_1^{15}\text{N}_1^{16}\text{O}_7^{18}\text{O}_1$) were summed. The theoretical relative abundance for each m/z ratio of
5 $^{\text{nat}}\text{Sm}$ -EDTA was then calculated by summing the values of each column. On the basis of these
6 calculated abundances, the resulting theoretical $^{\text{nat}}\text{Sm}$ -EDTA isotopic pattern appears to be
7 consistent with the experimental mass spectrum, as illustrated in Figure 1a and c.

8
9 By considering the range of natural abundance variations provided by IUPAC for H, C, N and O,¹⁹
10 the maximum impact on calculated abundance ratios was $\pm 1.4\%$ for the $^{\text{nat}}\text{Sm}$ -EDTA ratio of
11 432/438, with the species at $m/z = 432$ containing the less abundant ^{144}Sm isotope (3.1%). The
12 difference was lower than 0.1% for the other isotope ratios. These variations were therefore
13 considered to be negligible in this study. That being said, the theoretical bias, corresponding to the
14 difference between experimental $^{\text{nat}}\text{Sm}$ -EDTA abundance ratios and calculated $^{\text{nat}}\text{Sm}$ -EDTA
15 abundances ratios by convolution, was calculated for all abundance ratios of $^{\text{nat}}\text{Sm}$ -EDTA. This
16 theoretical bias was better than 3% with repeatability of 3% for results obtained by ESI-QqQ-MS,
17 and better than 1% with repeatability of 1% with the ESI-LIT-MS (data not shown). To determine the
18 $^{\text{nat}}\text{Sm}$ isotopic composition by deconvolution of the experimental $^{\text{nat}}\text{Sm}$ -EDTA mass spectra obtained
19 by ESIMS, the next step was to remove the isotopic contributions of H, C, N and O at each m/z ratio.
20 For this, a system of n equations with n unknowns, was defined from the abundance matrix (Table
21 3) and further solved. In the case of $^{\text{nat}}\text{Sm}$ -EDTA, n is equal to 7, which represents the atomic
22 abundances of the seven $^{\text{nat}}\text{Sm}$ isotopes. The H, C, N and O contributions for each m/z ratio were
23 calculated by dividing each row of the matrix by the atomic abundance of corresponding $^{\text{nat}}\text{Sm}$
24 isotopes. A new matrix including only the H, C, N and O isotopic contributions from EDTA was then
25 obtained (Table 4).

Table 4: H, C, N and O isotopic contribution matrix in the isotopic pattern of ^{nat}Sm-EDTA

View Article Online
DOI: 10.1039/D0JA00471E

H, C, N and O isotopic contributions	<i>m/z</i> ratio						
	432	435	436	437	438	440	442
¹⁴⁴ Sm	0.873	1.907×10 ⁻³	1.989×10 ⁻⁴	1.518×10 ⁻⁵	6.713×10 ⁻⁷	1.493×10 ⁻¹⁰	2.887×10 ⁻¹⁶
¹⁴⁷ Sm		0.873	0.105	2.0×10 ⁻²	1.907×10 ⁻³	1.518×10 ⁻⁵	2.077×10 ⁻⁸
¹⁴⁸ Sm			0.873	0.105	2.0×10 ⁻²	1.989×10 ⁻⁴	6.712×10 ⁻⁷
¹⁴⁹ Sm				0.873	0.105	1.907×10 ⁻³	1.518×10 ⁻⁵
¹⁵⁰ Sm					0.873	2.0×10 ⁻²	1.989×10 ⁻⁴
¹⁵² Sm						0.873	2.0×10 ⁻²
¹⁵⁴ Sm							0.873

The ^{nat}Sm isotope ratios were then determined from the measured intensities (*I*) of the ^{nat}Sm-EDTA isotopic pattern and the contribution matrix of the H, C, N, O isotopes at each *m/z* ratio, by defining a system of 7 equations, with the 7 unknowns being the atomic abundances of ^{nat}Sm isotopes.

For example, for *m/z* 432 and *m/z* 435 (Table 4 and Eq. 3):

$${}^{432}I = 0.873 \times {}^{144}A \text{ and } {}^{435}I = 1.907 \times 10^{-3} \times {}^{144}A + 0.873 \times {}^{147}A \quad (\text{Eq. 3})$$

The ^{nat}Sm isotope ratios were then determined by combining the obtained atomic abundances. An example is given below for the ¹⁴⁷Sm/¹⁴⁴Sm ratio (Eq. 4):

$$\frac{{}^{432}I}{{}^{435}I} = \frac{0.873 \times {}^{144}A}{1.907 \times 10^{-3} \times {}^{144}A + 0.873 \times {}^{147}A} \rightarrow \frac{{}^{147}A}{{}^{144}A} = \frac{0.873 - 1.907 \times 10^{-3} \times \frac{{}^{432}I}{{}^{435}I}}{0.873 \times \frac{{}^{432}I}{{}^{435}I}} \quad (\text{Eq. 4})$$

INTENSITIES MEASURED
ISOTOPE RATIO

SPECIES
ELEMENT

Since the deconvolution method developed does not depend on the Sm isotopic composition, it is particularly relevant for any applications in which non-natural isotopic abundances are involved.

Determination of isotopic composition of lanthanides contained in chemical species by ESIMS

The experimental mass spectra of ^{nat}Sm-EDTA (Figure 1a) were deconvoluted to obtain the isotopic pattern of ^{nat}Sm (Figure 1d). The results are given in Table 5, together with the reference isotope ratios of ^{nat}Sm, the trueness, calculated as the difference between experimental ^{nat}Sm isotope ratios obtained after deconvolution and the reference ^{nat}Sm isotope ratios, as well as the repeatability of the measurements.

Table 5: ^{nat}Sm isotope ratios determined after deconvolution of ^{nat}Sm -EDTA mass spectra acquired with ESI-QqQ-MS and ESI-LIT-MS. The measured ratios were determined based on the average of ten measurements. Trueness after deconvolution was calculated in comparison with the reference ^{nat}Sm isotope ratios obtained by TIMS¹³. Repeatability was expressed at $k=2$ after deconvolution.

^{nat}Sm isotope ratios		$^{144}\text{Sm}/^{150}\text{Sm}$	$^{147}\text{Sm}/^{150}\text{Sm}$	$^{148}\text{Sm}/^{150}\text{Sm}$	$^{149}\text{Sm}/^{150}\text{Sm}$	$^{152}\text{Sm}/^{150}\text{Sm}$	$^{154}\text{Sm}/^{150}\text{Sm}$
TIMS reference value ¹³		0.4194	2.0365	1.5257	1.8739	3.6173	3.0733
ESI-QqQ-MS	Average (n=10)	0.4062	1.9799	1.4976	1.8502	3.6264	3.0474
	Trueness (%)	-3.1	-2.8	-1.8	-1.3	0.3	-0.8
	Repeatability (%)	2.2	1.2	2.8	2.0	1.5	1.9
ESI-LIT-MS	Average (n=10)	0.4166	2.0376	1.5296	1.8718	3.6216	3.0860
	Trueness (%)	-0.7	0.1	0.3	-0.1	0.1	0.4
	Repeatability (%)	1.0	0.9	0.7	0.9	0.7	0.7

The bias before deconvolution, calculated as the difference between the experimental ^{nat}Sm -EDTA abundance ratios and the reference ^{nat}Sm isotope ratios, ranged between 8 and 24%. After deconvolution, the ^{nat}Sm isotope ratios were determined with a trueness better than 3.5% and a repeatability of about 3% for ESI-QqQ-MS, and a trueness better than 1.0% and a repeatability of about 1% for ESI-LIT-MS.

The same approach was applied to a double spike enriched in $^{147-149}\text{Sm}$ of known isotopic composition and complexed with EDTA. The isotopic composition of $^{147-149}\text{Sm}$ was then determined from the $^{147-149}\text{Sm}$ -EDTA mass spectra recorded with ESI-QqQ-MS and ESI-LIT-MS.

This double spike was selected since $^{147-149}\text{Sm}$ -EDTA leads to a more complex spectrum than ^{nat}Sm -EDTA for the less abundant Sm isotopes (Figures 1a and 3a).

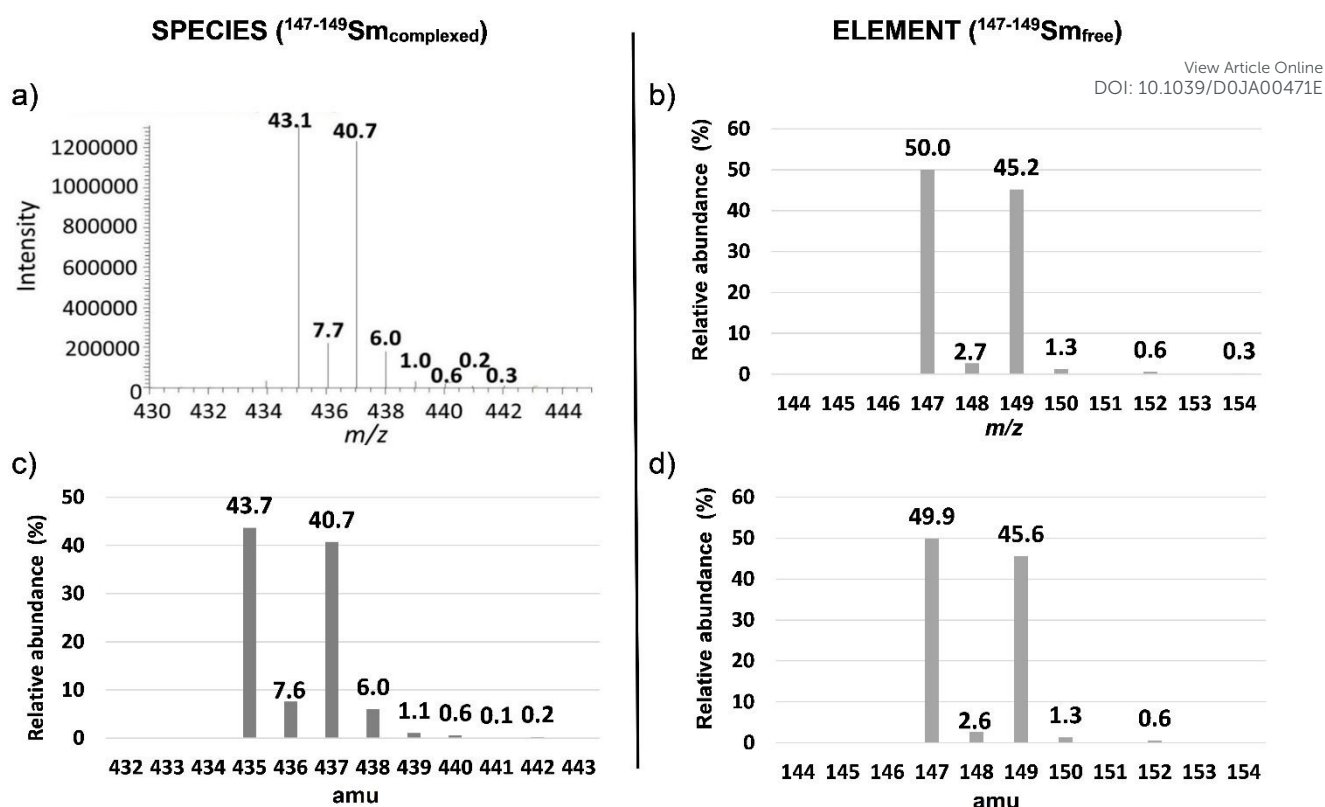


Figure 3: Isotopic patterns of $^{147-149}\text{Sm-EDTA}$ and $^{147-149}\text{Sm}$ a) experimental mass spectrum of $^{147-149}\text{Sm-EDTA}$ recorded by ESI-LIT-MS in full scan mode, b) reference $^{147-149}\text{Sm}$ isotopic pattern obtained by TIMS¹⁴, c) $^{147-149}\text{Sm-EDTA}$ isotopic pattern calculated with the Yergey convolution method¹⁷, d) $^{147-149}\text{Sm}$ isotopic pattern obtained by deconvolution of the experimental ESI mass spectrum of $^{147-149}\text{Sm-EDTA}$

In particular, the less abundant Sm isotope of $^{\text{nat}}\text{Sm}$ (^{144}Sm) led to 2.7% abundance at m/z 432 in the $^{\text{nat}}\text{Sm-EDTA}$ convoluted spectrum (Figure 1c). This mass was not impacted by the H, C, N and O isotopic contributions because it is associated with the lightest Sm isotope. The abundances in the $^{\text{nat}}\text{Sm-EDTA}$ spectrum ranging between 8.1 and 23.5% (Figure 1c) are associated with Sm isotopes with abundances ranging between 7.4 and 26.7% (Figure 1b). Conversely, there are two major ions with abundances of 43.7 and 40.7% at m/z 435 and m/z 437 in the $^{147-149}\text{Sm-EDTA}$ convoluted spectrum (Figure 3c). These peaks are related to ^{147}Sm and ^{149}Sm isotopes with abundances of 50.0 and 45.2% (Figure 3b). The other Sm isotopes showed much lower abundances (less than 2.7%) and were all significantly impacted by the H, C, N and O isotopic contributions. In particular, the relative abundances of ^{148}Sm and ^{150}Sm were 2.7% and 1.3% (Figure 3b), and 7.6% and 6% respectively for m/z 436 and m/z 438 in the $^{147-149}\text{Sm-EDTA}$ isotopic pattern (Figure 3c).

As the theoretical bias calculated with m/z 435 as reference was systematically positive with ESI-LIT-MS for the $^{148}\text{Sm-EDTA}/^{147}\text{Sm-EDTA}$ ratio and for all abundance ratios of $^{147-149}\text{Sm-EDTA}$ with ESI-QqQ-MS (data not shown), we attributed these interferences to the residual nitrates coming from the sample preparation. To remove such interference, corrections detailed in the experimental part were applied. After correction, the theoretical bias and the repeatability at $k = 2$ were better than 2% and 4% with ESI-QqQ-MS (data not shown), for all abundance ratios for which Sm isotope abundances were greater than 1%. With ESI-LIT-MS, the theoretical bias and the repeatability were better than 2% for all abundance ratios, except for the $^{152}\text{Sm-EDTA}/^{147}\text{Sm-EDTA}$ ratio, for which the theoretical bias was about 9%, because of the too low intensity of the signal. The experimental ESI-LIT-MS mass spectra of $^{147-149}\text{Sm-EDTA}$ (Figure 3a) were deconvoluted to obtain the $^{147-149}\text{Sm}$ isotopic composition (Figure 3d). Table 6 gives the isotope ratios of $^{147-149}\text{Sm}$ determined after deconvolution of mass spectra, the reference $^{147-149}\text{Sm}$ isotope ratios, the trueness and the repeatability of the measurements.

Table 6: $^{147-149}\text{Sm}$ isotope ratios determined after deconvolution of $^{147-149}\text{Sm-EDTA}$ mass spectra acquired with ESI-QqQ-MS and ESI-LIT-MS. The measured ratios were based on the average of three replicates of ten measurements. Trueness after deconvolution was calculated in comparison with the reference $^{147-149}\text{Sm}$ isotope ratios obtained by TIMS¹⁴. Repeatability is expressed at $k=2$ after deconvolution.

$^{147-149}\text{Sm}$ isotope ratios		$^{148}\text{Sm}/^{147}\text{Sm}$	$^{149}\text{Sm}/^{147}\text{Sm}$	$^{150}\text{Sm}/^{147}\text{Sm}$	$^{152}\text{Sm}/^{147}\text{Sm}$
TIMS reference value ¹⁴		0.0534	0.9035	0.0253	0.0113
ESI-QqQ-MS	Average ($n=3\times 10$)	0.0531	0.9135	0.0258	0.0061
	Trueness (%)	-0.6	1.1	2.0	-46.3
	Repeatability (%)	9.3	3.0	12.9	7.5
ESI-LIT-MS	Average ($n=3\times 10$)	0.0524	0.9136	0.0253	0.0125
	Trueness (%)	-2.0	1.1	0.3	10.4
	Repeatability (%)	1.8	0.2	2.5	2.1

The bias before deconvolution for the major $^{149}\text{Sm-EDTA}/^{147}\text{Sm-EDTA}$ abundance ratio was around 4% with the two ESI instruments, whereas it was between 25% and 450% for the minor abundance

1 ratios. After deconvolution, we achieved a trueness better than 2% with the two instruments, except
2 for the $^{152}\text{Sm}/^{147}\text{Sm}$ ratio for which the ^{152}Sm abundance was 0.6% (Figure 3d). For this ratio,
3 View Article Online
DOI: 10.1039/D0JA00471E
4 trueness was worse than 10%. With ESI-QqQ-MS, the repeatability was 3% for the major
5 $^{149}\text{Sm}/^{147}\text{Sm}$ ratio, while it was about 10% for the other ratios. With ESI-LIT-MS, the repeatability was
6 better than 2.5% for all isotope ratios. These results confirm the validity of all the isotopic
7 measurements we performed with commercial ESIMS instruments as well as the readily
8 implementable deconvolution method, for isotopes of relative abundances greater than 1% in
9 samples. The $^{147-149}\text{Sm}$ isotope ratios were determined by ESI-QqQ-MS and ESI-LIT-MS with a
10 trueness better than 3% for Sm isotope ratios ranging between 0.025 and 0.9 with isotope
11 abundances as low as 1.3%. This is true despite the strong impact of the H, C, N and O isotopic
12 contributions from adjacent major peaks 20 to 40 times more intense.

13 We further carried out isotopic measurements starting with ESI mass spectra of chemical species
14 containing another lanthanide ($^{\text{nat}}\text{Nd-EDTA}$), another ligand ($^{\text{nat}}\text{Sm-DTPA}$) and different lanthanide
15 and ligand ($^{\text{nat}}\text{Nd-DTPA}$). The isotope ratios of $^{\text{nat}}\text{Nd}$ and $^{\text{nat}}\text{Sm}$ were then determined by applying the
16 deconvolution method to the associated lanthanide complexes and compared to reference ratios of
17 the free lanthanides. The isotope ratios of $^{\text{nat}}\text{Nd}$ determined after deconvolution of $^{\text{nat}}\text{Nd-DTPA}$ mass
18 spectra (Figure S1), the reference $^{\text{nat}}\text{Nd}$ isotope ratios, the trueness and the repeatability of the
19 measurements are given below in Table 7, while the results obtained for $^{\text{nat}}\text{Nd-EDTA}$ and $^{\text{nat}}\text{Sm-}$
20 DTPA are provided in Tables S1 and S2, as well as in figures S2 and S3.
21
22
23
24
25
26
27
28
29
30
31
32
33
34
35
36
37
38
39
40
41
42
43
44
45
46
47
48
49
50
51
52
53
54
55
56
57
58
59
60

Table 7: ^{nat}Nd isotope ratios determined after deconvolution of ^{nat}Nd -DTPA mass spectra acquired with ESI-QqQ-MS and ESI-LIT-MS. The measured ratios were based on the average of ten measurements. Trueness after deconvolution was calculated in comparison with the reference ^{nat}Nd isotope ratios obtained by TIMS¹³. Repeatability was expressed at k=2 after deconvolution.

^{nat}Nd isotope ratios		$^{142}\text{Nd}/^{144}\text{Nd}$	$^{143}\text{Nd}/^{144}\text{Nd}$	$^{145}\text{Nd}/^{144}\text{Nd}$	$^{146}\text{Nd}/^{144}\text{Nd}$	$^{148}\text{Nd}/^{144}\text{Nd}$	$^{150}\text{Nd}/^{144}\text{Nd}$
TIMS reference value ¹³		1.1397	0.5110	0.3487	0.7233	0.2430	0.2382
ESI-QqQ-MS	Average (n=10)	1.1304	0.5090	0.3479	0.7205	0.2444	0.2391
	Trueness (%)	-0.8	-0.4	-0.2	-0.4	0.6	0.4
	Repeatability (%)	2.1	2.1	2.1	1.4	2.1	2.4
ESI-LIT-MS	Average (n=10)	1.1225	0.5089	0.3451	0.7228	0.2432	0.2366
	Trueness (%)	-1.5	-0.4	-1.0	-0.1	0.1	-0.7
	Repeatability (%)	0.3	0.4	0.5	0.3	0.3	0.4

For all abundance ratios of ^{nat}Nd -DTPA measured by ESI-QqQ-MS and ESI-LIT-MS, a bias between 0 and 30% was obtained before deconvolution in comparison with reference ^{nat}Nd isotope ratios obtained by TIMS¹³. After deconvolution of the ^{nat}Nd -DTPA mass spectra, the ^{nat}Nd isotope ratios were determined with a trueness better than 1% and a repeatability of around 2% with ESI-QqQ-MS, and a trueness better than 1.5% and a repeatability of around 0.5% with ESI-LIT-MS (Table 7). These results indicate that the performance of ^{nat}Nd isotope ratio measurements obtained from ESI mass spectra of ^{nat}Nd -DTPA are very good and similar to those measured for the ^{nat}Sm -EDTA species, by retaining the same experimental parameters.

By deconvolution of the mass spectra of ^{nat}Nd -EDTA and ^{nat}Sm -DTPA, the isotope ratios of the ^{nat}Ln were determined with a trueness better than 3.0% and a repeatability of around 2.5% with ESI-QqQ-MS, and a trueness better than 2.5% and a repeatability of around 0.5% with ESI-LIT-MS (Tables S1 and S2 and Figures S2 and S3). Overall, we were able to demonstrate that the substitution of Sm by Nd in the EDTA or DTPA chemical species has no impact either on the quality of the isotopic measurements with the two ESIMS instruments, or on the performance of the deconvolution method that we developed.

1
2 This work was carried out using model samples but can be performed with more complex samples,
3
4 by coupling a separation step to ESIMS, to isolate the chemical species and the potential interferences
5
6 before the analysis step.
7
8
9

View Article Online
DOI: 10.1039/D0JA00471E

10 CONCLUSION

11
12 The aim of the present work was to determine the isotopic composition of elements contained in
13
14 chemical species, by electrospray mass spectrometry. In particular, the isotopic composition of
15
16 natural and non-natural Sm and natural Nd contained in EDTA and DTPA complexes, were
17
18 determined using two different mass spectrometers. To meet this aim, we developed a user-friendly
19
20 deconvolution method to directly determine the Ln isotopic composition based on ESI mass spectra
21
22 of the associated chemical species, by removing the isotopic contributions of the atoms from the
23
24 ligand without performing fragmentations experiments by tandem mass spectrometry. By applying
25
26 the deconvolution method to the mass spectra of Sm-EDTA species containing natural and enriched
27
28 samarium, a trueness and a repeatability globally better than 3% were obtained for all isotope ratios
29
30 of Sm with isotope abundances greater than 1%, using ESI-QqQ-MS and ESI-LIT-MS. The
31
32 performance of the $^{147-149}\text{Sm}$ -EDTA abundance ratio measurements and deconvolution method
33
34 demonstrated the approach applicability for non-natural sample analysis; including low-abundance
35
36 isotopes strongly impacted by H, C, N, and O isotopic contributions from the major neighbouring
37
38 isotopes. The deconvolution method was also successfully applied to other Ln-polyaminocarboxylic
39
40 species such as $^{\text{nat}}\text{Nd}$ -EDTA, $^{\text{nat}}\text{Sm}$ -DTPA and $^{\text{nat}}\text{Nd}$ -DTPA, leading to similar performance of
41
42 trueness and repeatability. This approach can be extended to the isotopic characterization of
43
44 elements contained in any chemical species by electrospray mass spectrometry, and appears
45
46 therefore to be promising for the use this technique by its own for elemental speciation analysis. The
47
48 implementation of this approach to LC-ESIMS coupling is of great interest for the comprehensive
49
50 speciation study of elements in various fields. Such comprehensive speciation is of great concern in
51
52 applications associated with the nuclear fuel cycle for the development of spent fuel treatment
53
54 processes, in nuclear toxicology to study the effect of radioelements at the cellular and molecular
55
56 level and design specific decorporation agents, in geosciences to determine the distribution
57
58
59
60

1
2 processes of contaminants chelated to different organic ligands in environmental compartments and
3
4 in life sciences to better understand the mechanisms underlying the toxicity of metals.
5
6
7

View Article Online
DOI: 10.1039/D0JA00471E

8 **CONFLICT OF INTEREST**

9
10 There is no conflict of interest to declare.
11
12
13

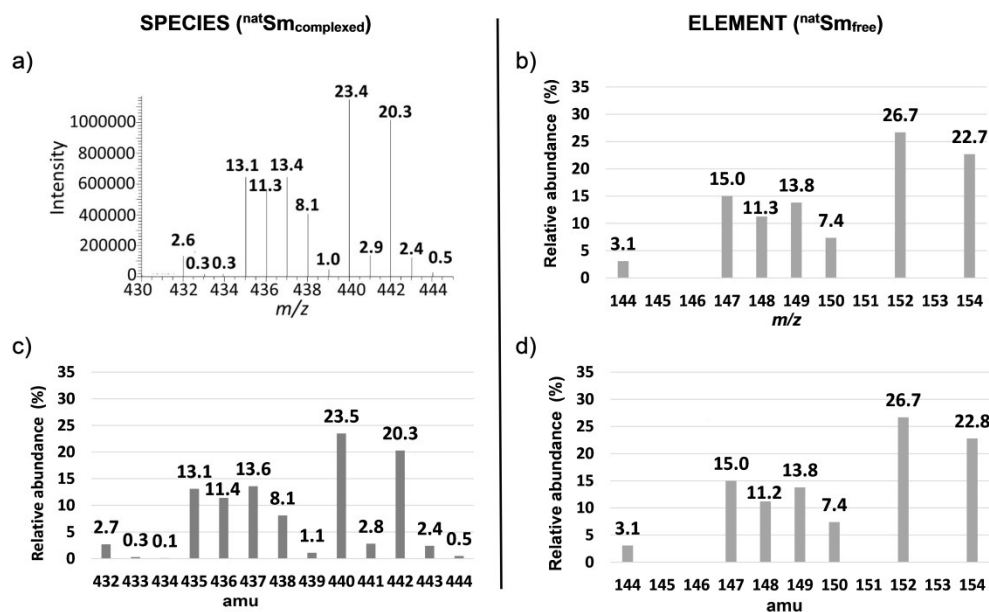
14 **ACKNOWLEDGMENTS**

15
16 The authors would like to acknowledge the CEA for its financial support.
17
18
19
20
21
22
23
24
25
26
27
28
29
30
31
32
33
34
35
36
37
38
39
40
41
42
43
44
45
46
47
48
49
50
51
52
53
54
55
56
57
58
59
60

REFERENCES:

1. D. M. Templeton, F. Ariese, R. Cornelis, L.-G. Danielsson, H. Muntau, H. P. Van Leeuwen and R. Lobinski, *Pure Appl. Chem.*, 2000, **72**, 1453-1470.
2. D. M. Templeton and H. Fujishiro, *Coord. Chem. Rev.*, 2017, **352**, 424-431.
3. EGADSNF, Paris, France. OECD, NEA/NSC/WPNCS/DOC, 2011, **5**.
4. D. Schaumlöffel and A. Tholey, *Anal. Bioanal. Chem.*, 2011, **400**, 1645-1652.
5. S. Miah, S. Fukiage, Z. A. Begum, T. Murakami, A. S. Mashio, I. M. M. Rahman and H. Hasegawa, *J. Chromatogr. A*, 2020, **1630**, 461528.
6. L. Beuvier, C. Bresson, A. Nonell, L. Vio, N. Henry, V. Pichon and F. Chartier, *RSC Adv.*, 2015, **5**, 92858-92868.
7. M. J. Keith-Roach, *Anal. Chim. Acta*, 2010, **678**, 140-148.
8. R. Jirásko and M. Holčápek, *Mass Spectrom. Rev.*, 2011, **30**, 1013-1036.
9. C. Shiea, Y. L. Huang, S. C. Cheng, Y. L. Chen and J. Shiea, *Anal. Chim. Acta*, 2017, **968**, 50-57.
10. M. E. Ketterer and J. P. Guzowski, *Anal. Chem.*, 1996, **68**, 883-887.
11. M. C. B. Moraes, J. G. A. Brito Neto and C. L. do Lago, *J. Anal. At. Spectrom.*, 2001, **16**, 1259-1265.
12. C. Liu, B. Hu, J. Shi, J. Li, X. Zhang and H. Chen, *J. Anal. At. Spectrom.*, 2011, **26**, 2045-2051.
13. J. C. Dubois, G. Retali and J. Cesario, *Int. J. Mass Spectrom. Ion Process.*, 1992, **120**, 163-177.
14. M. Bourgeois, H. Isnard, A. Gourgiotis, G. Stadelmann, C. Gautier, S. Mialle, A. Nonell and F. Chartier, *J. Anal. At. Spectrom.*, 2011, **26**, 1660-1666.
15. J. Kragten, *Analyst*, 1994, **119**, 2161-2165.
16. K. Scheubert, F. Hufsky and S. Böcker, *J. Cheminform*, 2013, **5**, 1-24.
17. J. A. Yergey, *Int. J. Mass spectrom. Ion Physics*, 1983, **52**, 337-349.
18. M. Berglund and M. E. Wieser, *Pure Appl. Chem.*, 2011, **83**, 397-410.
19. J. Meija, T. B. Coplen, M. Berglund, W. A. Brand, P. De Bièvre, M. Gröning, N. E. Holden, J. Irrgeher, R. D. Loss, T. Walczyk and T. Prohaska, *Pure Appl. Chem.*, 2016, **88**, 293-306.

View Article Online
DOI: 10.1039/C6AY0471E



Isotopic patterns of ^{nat}Sm -EDTA and ^{nat}Sm a) experimental mass spectrum of ^{nat}Sm -EDTA recorded by ESI-LIT-MS in full scan mode, b) reference ^{nat}Sm isotopic pattern obtained by TIMS¹³, c) ^{nat}Sm -EDTA isotopic pattern calculated with the Yergey convolution method¹⁷ d) ^{nat}Sm isotopic pattern obtained by deconvolution of the experimental ESI mass spectrum of ^{nat}Sm -EDTA

1191x760mm (120 x 120 DPI)

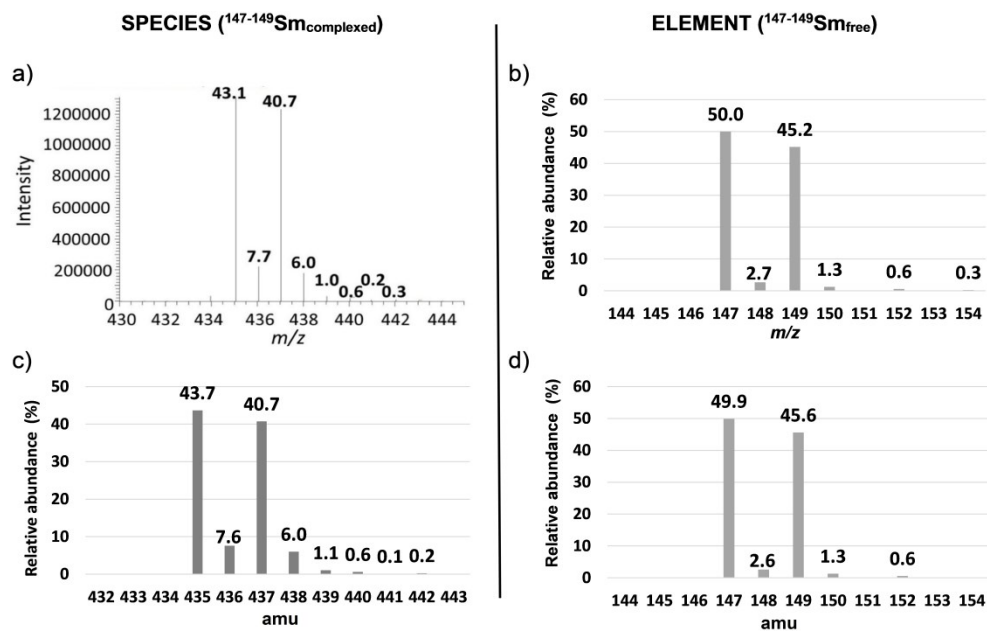
1
2
3
4
5
6
7
8
9
10
11
12
13
14
15
16
17
18
19
20
21
22
23
24
25
26
27
28
29
30
31
32
33
34
35
36
37
38
39
40
41
42
43
44
45
46
47
48
49
50
51
52
53
54
55
56
57
58
59
60

Carbon					
Number of ¹²C	Number of ¹³C	m/z	Abundance	Abundance (ppm)	
10	0	120	0.898	898008	
9	1	121	0.097	97126	
8	2	122	0.005	4727	
7	3	123	1.10 ⁻⁴	136	
6	4	124	3.10 ⁻⁶	3	
5	5	125	3.10 ⁻⁸	3.10 ⁻²	

Hydrogen					
Number of ¹H	Number of ²H	m/z	Abundance	Abundance (ppm)	
12	0	12	0.999	998621	
11	1	13	0.001	1378	
10	2	14	9.10 ⁻⁷	0.9	

Atomic abundance of carbon and hydrogen isotopic permutations for deprotonated EDTA (C₁₀H₁₂N₂O₈)

283x184mm (120 x 120 DPI)



Isotopic patterns of $^{147-149}\text{Sm}$ -EDTA and $^{147-149}\text{Sm}$ a) experimental mass spectrum of $^{147-149}\text{Sm}$ -EDTA recorded by ESI-LIT-MS in full scan mode, b) reference $^{147-149}\text{Sm}$ isotopic pattern obtained by TIMS¹⁴, c) $^{147-149}\text{Sm}$ -EDTA isotopic pattern calculated with the Yerger convolution method¹⁷, d) $^{147-149}\text{Sm}$ isotopic pattern obtained by deconvolution of the experimental ESI mass spectrum of $^{147-149}\text{Sm}$ -EDTA

1183x774mm (120 x 120 DPI)